SLAC–PUB–95–6997
October 1995

Measurements of the Q^2-Dependence of the Proton and Deuteron Spin Structure Functions g_1^p and g_1^d

The E143 Collaboration[⋆]

K. Abe,[15] T. Akagi,[12,15] P. L. Anthony,[12] R. Antonov,[11] R. G. Arnold,[1] T. Averett,[16] H. R. Band,[17] J. M. Bauer,[7] H. Borel,[5] P. E. Bosted,[1] V. Breton,[3] J. Button-Shafer,[7] J. P. Chen,[16] T. E. Chupp,[8] J. Clendenin,[12] C. Comptour,[3] K. P. Coulter,[8] G. Court,[12,*] D. Crabb,[16] M. Daoudi,[12] D. Day,[16] F. S. Dietrich,[6] J. Dunne,[1] H. Dutz,[12,**] R. Erbacher,[12,13] J. Fellbaum,[1] A. Feltham,[2] H. Fonvieille,[3] E. Frlez,[16] D. Garvey,[9] R. Gearhart,[12] J. Gomez,[4] P. Grenier,[5] K. A. Griffioen,[11,†] S. Hoibraten,[16,§] E. W. Hughes,[12] C. Hyde-Wright,[10] J. R. Johnson,[17] D. Kawall,[13] A. Klein,[10] S. E. Kuhn,[10] M. Kuriki,[15] R. Lindgren,[16] T. J. Liu,[16] R. M. Lombard-Nelsen,[5] J. Marroncle,[5] T. Maruyama,[12] X. K. Maruyama,[9] J. McCarthy,[16] W. Meyer,[12,**] Z.-E. Meziani,[13,14] R. Minehart,[16] J. Mitchell,[4] J. Morgenstern,[5] G. G. Petratos,[12,‡] R. Pitthan,[12] D. Pocanic,[16] C. Prescott,[12] R. Prepost,[17] P. Raines,[11] B. Raue,[10] D. Reyna,[1] A. Rijllart,[12,††] Y. Roblin,[3] L. S. Rochester,[12] S. E. Rock,[1] O. A. Rondon,[16] I. Sick,[2] L. C. Smith,[16] T. B. Smith,[8] M. Spengos,[1] F. Staley,[5] P. Steiner,[2] S. St.Lorant,[12] L. M. Stuart,[12] F. Suekane,[15] Z. M. Szalata,[1] H. Tang,[12] Y. Terrien,[5] T. Usher,[12] D. Walz,[12] J. L. White,[1] K. Witte,[12] C. C. Young,[12] B. Youngman,[12] H. Yuta,[15] G. Zapalac,[17] B. Zihlmann,[2] D. Zimmermann[16]

[1]The American University, Washington, D.C. 20016
[2]Institut für Physik der Universität Basel, CH–4056 Basel, Switzerland
[3]LPC IN2P3/CNRS, University Blaise Pascal, F–63170 Aubiere Cedex, France
[4]CEBAF, Newport News, Virginia 23606
[5]DAPNIA-Service de Physique Nucleaire Centre d'Etudes de Saclay, F–91191 Gif/Yvette, France
[6]Lawrence Livermore National Laboratory, Livermore, California 94550
[7]University of Massachusetts, Amherst, Massachusetts 01003
[8]University of Michigan, Ann Arbor, Michigan 48109
[9]Naval Postgraduate School, Monterey, California 93943
[10]Old Dominion University, Norfolk, Virginia 23529
[11]University of Pennsylvania, Philadelphia, Pennsylvania 19104
[12]Stanford Linear Accelerator Center, Stanford, California 94309
[13]Stanford University, Stanford, California 94305
[14]Temple University, Philadelphia, Pennsylvania 19122
[15]Tohoku University, Sendai 980, Japan
[16]University of Virginia, Charlottesville, Virginia 22901
[17]University of Wisconsin, Madison, Wisconsin 53706

Submitted to Physics Letters B

[⋆]Work supported in part by Department of Energy contract DE–AC03–76SF00515 (SLAC), and by other Department of Energy contracts for CEBAF, LLNL, ODU, Stanford, Virginia and Wisconsin; by the National Science Foundation (American, Massachusetts, Michigan, ODU, and U. Penn.); by the Schweizersche Nationalfonds (Basel); by the Commonwealth of Virginia (Virginia); by the Centre National de la Recherche Scientifique and the Commissariat a l'Energie Atomique (French groups); and by the Japanese Ministry of Education, Science, and Culture (Tohoku).
[*]Permanent address: Oliver Lodge Lab, University of Liverpool, Liverpool, U.K.
[**]Permanent address: University of Bonn, D-53113 Bonn, Germany.
[†]Present address: College of William and Mary, Williamsburg, Virginia 23187.
[§]Permanent address: FFIYM, P.O. Box 25, N-2007 Kjeller, Norway.
[‡]Present address: Kent State University, Kent, Ohio 44242.
[††]Permanent address: CERN, 1211 Geneva 23, Switzerland.

ABSTRACT

The ratio g_1/F_1 has been measured over the range $0.03 < x < 0.6$ and $0.3 < Q^2 < 10$ (GeV/c)^2 using deep-inelastic scattering of polarized electrons from polarized protons and deuterons. We find g_1/F_1 to be consistent with no Q^2-dependence at fixed x in the deep-inelastic region $Q^2 > 1$ (GeV/c)^2. A trend is observed for g_1/F_1 to decrease at lower Q^2. Fits to world data with and without a possible Q^2-dependence in g_1/F_1 are in agreement with the Bjorken sum rule, but Δq is substantially less than the quark-parton model expectation.

The longitudinal spin-dependent structure function $g_1(x, Q^2)$ for deep-inelastic lepton-nucleon scattering has become increasingly important in unraveling the quark and gluon spin structure of the proton and neutron. The g_1 structure function depends both on x, the fractional momentum carried by the struck parton, and on Q^2, the four-momentum transfer squared of the virtual photons used as a probe of nucleon structure. Of particular interest are the fixed-Q^2 integrals $\Gamma_1^p(Q^2) = \int_0^1 g_1^p(x, Q^2)dx$ for the proton and $\Gamma_1^n(Q^2) = \int_0^1 g_1^n(x, Q^2)dx$ for the neutron. These integrals are directly related to the net quark helicity Δq in the nucleon. Measurements of Γ_1^p [1–5], Γ_1^d [6–7], and Γ_1^n [8] have found $\Delta q \approx 0.3$, significantly less than a prediction [9] that $\Delta q = 0.58$ assuming zero net strange quark helicity and SU(3) flavor symmetry in the baryon octet. A fundamental sum rule originally derived from current algebra by Bjorken [10] predicts the difference $\Gamma_1^p(Q^2) - \Gamma_1^n(Q^2)$. Recent measurements are in agreement with this sum rule prediction when perturbative QCD (pQCD) corrections [11] are included.

There are two main reasons for measuring g_1 over a wide range of x and Q^2. The first is that experiments make measurements at fixed beam energies rather than at fixed Q^2. To evaluate first moment integrals of $g_1(x, Q^2)$ at constant Q^2 [typically between 2 and 10 (GeV/c)^2], extrapolations are needed. Data at low x are at lower Q^2 than desired

[as low as 1 (GeV/c)^2], while data at high x are at higher Q^2 [up to 80 (GeV/c)^2]. Data at multiple beam energies allow for a measurement of the kinematic dependence of g_1, rather than relying on model-dependent extrapolations for the moment determinations.

The second motivation is that the kinematic dependence of g_1 can be used to obtain the underlying nucleon polarized quark and gluon distribution functions. According to the GLAP equations [12], g_1 is expected to evolve logarithmically with Q^2, increasing with Q^2 at low x, and decreasing with Q^2 at high x. A similar Q^2-dependence has been observed in the spin-averaged structure functions $F_1(x, Q^2)$ and $F_2(x, Q^2)$. For reference, in changing Q^2 from 2 to 10 (GeV/c)^2, F_1 decreases by 40% for $x \approx 0.5$, but increases by the same amount for $x \approx 0.035$ [13,14]. Since the GLAP equations are similar for F_1 and g_1, the Q^2 dependence of g_1 is expected to be similar to that of F_1, but the precise behavior is sensitive to the underlying spin-dependent quark and gluon distribution functions. Fits to polarized quark and gluon distribution functions have been made [15–19] using leading-order (LO) GLAP equations and data for $g_1(x, Q^2)$. Because of the limited Q^2 range and statistical precision of the data, constraints from QCD counting rules and Regge theory on the x-dependence have generally been imposed. Recently, fits have also been made [20,21] using next-to-leading-order (NLO) GLAP equations [17]. The results indicate that NLO fits are more sensitive to the strength of the polarized gluon distribution function $\Delta G(x, Q^2)$ than LO fits.

The theoretical interpretation of g_1 at low Q^2 is complicated by higher twist contributions not embodied in the GLAP equations. These terms are expected to be proportional to $C(x)/Q^2$, $D(x)/Q^4$, etc., where $C(x)$ and $D(x)$ are unknown functions. Higher twist contributions to the first moments Γ_1^p and Γ_1^n have been estimated to be only a few percent [22] for $Q^2 > 3$ (GeV/c)^2, but very little is known about their strength as a function of x.

In this Letter we study the Q^2 dependence of g_1 by supplementing our previously published results for g_1^p [5], g_1^d [7], and g_2^p and g_2^d [24] measured at average incident

electron beam energy E of 29.1 GeV with data for g_1^p and g_1^d at beam energies of 9.7 and 16.2 GeV. Data at all energies were taken at scattering angles of 4.5° and 7°. The ratio of polarized to unpolarized structure functions was determined from measured longitudinal asymmetries $A_\parallel$ using

$$g_1/F_1 = A_\parallel/d + (g_2/F_1)[(2Mx)/(2E-\nu)] \ , \tag{1}$$

where $d = [(1-\epsilon)(2-y)]/\{y[1+\epsilon R(x,Q^2)]\}$, $y = \nu/E$, $\nu = E - E'$, E' is the scattered electron energy, $\epsilon^{-1} = 1 + 2[1+\gamma^{-2}]\tan^2(\theta/2)$, $\gamma^2 = Q^2/\nu^2$, θ is the electron scattering angle, M is the nucleon mass, and $R(x,Q^2) = [F_2(x,Q^2)(1+\gamma^2)]/[2xF_1(x,Q^2)] - 1$ is typically 0.2 for the kinematics of this experiment [14]. For the contribution of the transverse spin structure function g_2 we used the twist-two model of Wandzura and Wilczeck (g_2^{WW}) [23]

$$g_2(x,Q^2) = -g_1(x,Q^2) + \int_x^1 g_1(\xi,Q^2)d\xi/\xi \ , \tag{2}$$

evaluated with g_1 based on a global fit to the virtual photon asymmetry A_1 (see fits V, Table I). The g_1 and g_2 structure functions are related to A_1 (which is bounded by $|A_1| < 1$) by $A_1 = (g_1/F_1) - \gamma^2(g_2/F_1)$. The g_2^{WW} model is in good agreement with our g_2 data at $E = 29$ GeV [24], the only energy at which both $A_\parallel$ and the transverse asymmetry $A_\perp$ were measured. Using other reasonable models for g_2 (such as $g_2 = 0$) has relatively little impact on the results for g_1 due to the factor $2Mx/(2E-\nu)$ in Eq. 1.

The data analysis was essentially identical to that reported for the 29 GeV data [5,7], with $A_\parallel$ calculated from the difference over the sum of rates for scattering longitudinally polarized electrons with spin either parallel or anti-parallel to polarized protons or deuterons in a cryogenic ammonia target. The most important corrections made were for the beam polarization (typically 0.85 ± 0.02), target polarization (typically 0.65 ± 0.017 for NH_3, 0.25 ± 0.011 for ND_3), fraction of polarizable nucleons (0.12 to 0.17 for NH_3, 0.22 to 0.24 for ND_3), and for contributions from polarized nitrogen atoms. Radiative corrections were calculated [25] using iterated global fits to all data (see fits V in Table I).

The data at 29 GeV used here differ slightly from our previously published results [5,7] due to the new radiative corrections, the inclusion of more data runs, and improved measurements of the polarization of the target and beam. Data in the it resonance region defined by missing mass $W < 1.8$ GeV were not included in the present analysis, but those for Q^2 below the traditional deep-inelastic cutoff of $Q^2 = 1$ (GeV/c)^2 were kept.

The results for g_1^p/F_1^p and g_1^d/F_1^d are shown in Figs. 1 and 2, respectively, at eight values of x, and are listed in Table II. We display the ratio g_1/F_1 since it is closer to our measured asymmetries than g_1 alone, and because g_1 and F_1 are expected theoretically to have a similar Q^2 dependence, so that differences are emphasized in the ratio. Data from other experiments [1–4,6] are plotted using published longitudinal asymmetries $A_\parallel$ and the same model for $R(x, Q^2)$ [14] and g_2 [23] as for the present data. Improved radiative corrections have been applied to the E80 [1] and E130 [2] results. Only statistical errors have been plotted. For the present experiment, most systematic errors (beam polarization, target polarization, fraction of polarizable nucleons in the target) for a given target are common to all data and correspond to an overall normalization error of about 5% for the proton data and 6% for the deuteron data. The remaining systematic errors (radiative corrections, model uncertainties for $R(x, Q^2)$, resolution corrections) vary smoothly with x in a locally correlated fashion, ranging from a few percent for moderate x bins, up to 15% for the highest and lowest x bins at $E = 29$ GeV. For all data, the statistical errors dominate over the point-to-point systematic error.

The most striking feature of the data is that g_1/F_1 is approximately independent of Q^2 at fixed x, although there is a noticeable trend for the ratio to decrease for $Q^2 < 1$ (GeV/c)^2. To quantify the possible significance of this trend, we made two fits to the data. The first fit is motivated by possible differences in the twist-4 contributions to g_1 and F_1. We fit the data in each x bin with the form $g_1/F_1 = a(1+C/Q^2)$. The results for the C coefficients are shown in Fig. 3 for all Q^2 [$Q^2 > 0.3$ (GeV/c)^2] (circles) and for $Q^2 > 1$ (GeV/c)^2 (squares). The coefficients indicate significantly negative values for C

at intermediate values of x for the fits over all Q^2. The errors are much larger when data with $Q^2 < 1$ (GeV/c)^2 are excluded, and the resulting coefficients are consistent with no Q^2-dependence to g_1/F_1 ($C = 0$). There is no evidence for a significant x-dependence to C. Another fit to the data in each x bin used the form $g_1/F_1 = a[1 + C\ln(1/Q^2)]$, motivated by looking for differences in the logarithmic evolution of g_1 and F_1. Again, the C coefficients tend to be less than zero when no Q^2 cut is applied. The present data do not have sufficient precision to distinguish between a logarithmic and power law Q^2 dependence, but can rule out large differences between the Q^2-dependence of g_1 and F_1, especially for $Q^2 > 1$ (GeV/c)^2.

Shown in Figs. 1 and 2 as the dot-dashed curves are the low-Q^2 predictions from a representative global NLO pQCD fit [20] to all proton and deuteron data excluding those at the 9.7 GeV and 16.2 GeV beam energies of this experiment. This group [20] finds considerably less Q^2 dependence to g_1/F_1 when a *minimal* polarized gluon strength is used than when a *maximal* strength is chosen. Another group has made NLO pQCD fits to proton, deuteron, and neutron data using different constraints on the underlying parton distribution functions [21], examining the sensitivity to SU(3) symmetry breaking in the baryon β decays. The results for their *standard* set are shown as the dotted curves in Figs. 1 and 2. Both [20] and [21] predict that g_1^p/F_1^p increases with Q^2 in the moderate x range ($0.03 < x < 0.3$), in agreement with the trend of our data when the $E = 9.7$ and $E = 16.2$ results (not included in their fits) are considered.

We also performed simple global fits to the data, both in order to have a practical parametrization (needed, for example, in making radiative corrections to the data), and to examine the possible effects of Q^2 dependence on the first moments Γ_1. Data points from SMC [4,6] at $x < 0.035$, not shown in Figs. 1 and 2, were included in the fits. The first fits are of the Q^2-independent form $g_1/F_1 = ax^\alpha(1 + bx + cx^2)$, with the constraint that $A_1 = g_1/F_1 - \gamma^2 g_2^{WW}/F_1 \to 1$ for $x \to 1$ at $Q^2 = 2$ (GeV/c)^2. As can be seen in Table I (case I), the fits to all the proton and deuteron data are acceptable (combined

$\chi^2 = 125$ for 104 d.f.), but the fits systematically lie above the lowest Q^2 points. The fits are improved ($\chi^2 = 94$ for 82 d.f.) by excluding the data for $Q^2 < 1$ (GeV/c)^2 (case II in Table I and dashed curves in Figs. 1 and 2). Better fits are obtained by introducing an overall multiplicative correction term of the form $(1 + C/Q^2)$ to account for the low Q^2 data ($\chi^2 = 104$ for 102 d.f.), as shown by the solid lines in Figs. 1 and 2 (case III in Tabl I). Using an x-independent value of C is reasonable given the results shown in Fig. 3. We examined an alternate correction term of the form $[1 + C\ln(1/Q^2)]$ (case IV in Table I) which shows an intermediate level of improvement ($\chi^2 = 113$ for 102 d.f.). We also examined the Q^2-dependence of A_1, extracted from measured values of $A_\parallel$ and using the g_2^{WW} model for g_2. The x coefficients listed in Table I (case V) are somewhat different from the g_1/F_1 fits, but the C coefficients remain negative. Thus both A_1 and g_1/F_1 indicate a significant tendency to decrease at low Q^2 when the low Q^2 data are included in the fits.

We have evaluated the first moments Γ_1^p and Γ_1^d, and the corresponding results for $\Gamma_1^p - \Gamma_1^n$, using the Q^2-independent fits II ($Q^2 > 1$ (GeV/c)^2) and the Q^2-dependent fits III (all Q^2) shown in Table I. A global fit [13,14] was used for F_1 to obtain g_1 from g_1/F_1. The results for $\Gamma_1^p - \Gamma_1^n$ are shown as a function of Q^2 as the lower (fit II) and upper (fit III) bands in Fig. 4, where the width of the band reflects the combined statistical and systematic error estimate. Both fits are in reasonable agreement with the Bjorken sum rule, shown as the solid curve, evaluated using $\alpha_s(Q^2)$ evolved in Q^2 from $\alpha_s(M_Z) = 0.117 \pm 0.005$ [26] for the QCD corrections [11] taken to third order in α_s. Alternatively, if we assume the sum rule is correct, we can use the measured $\Gamma_1^p(Q^2) - \Gamma_1^n(Q^2)$ to determine the strong coupling α_s. The case II (Q^2-independent g_1/F_1) fits to the proton and deuteron data integrated at $Q^2 = 3$ (GeV/c^2) yield $\alpha_s(M_Z) = 0.119^{+0.007}_{-0.019}$, while the case III ($Q^2$-dependent g_1/F_1) fits yield $\alpha_s(M_Z) = 0.113^{+0.011}_{-0.035}$, both in agreement with the world average result of 0.117.

We have examined the sensitivity to the possible Q^2 dependence of g_1/F_1 of the net quark helicity Δq extracted from global fits to the data. We computed Δq using [27]

$$\Delta q = \frac{9}{c_s(Q^2)}\Big[\Gamma_1^p(Q^2) - \Big(\frac{F+D}{12} + \frac{3F-D}{36}\Big)c_{ns}(Q^2)\Big] \ , \tag{3}$$

with $F+D = 1.2573 \pm 0.0028$ [26], $F/D = 0.575 \pm 0.016$ [27], extracted assuming SU(3) flavor symmetry in the baryon octet. The singlet and non-singlet QCD correction factors $c_s(Q^2)$ and $c_{ns}(Q^2)$ are given in [11,28]. At $Q^2 = 3$ (GeV/c)^2, we obtain $\Delta q = 0.34 \pm 0.09$ for global proton fit II, and $\Delta q = 0.36 \pm 0.10$ for proton fit III, somewhat higher than $\Delta q = 0.27 \pm 0.10$, obtained using the previous analysis of the E143 $E = 29$ GeV data only [5], which assumed g_1/F_1 independent of Q^2. For the deuteron fits, we used

$$\Delta q = \frac{9}{c_s(Q^2)}\Big[\frac{\Gamma_1^d(Q^2)}{1-1.5\omega_d} - \Big(\frac{3F-D}{36}\Big)c_{ns}(Q^2)\Big] \ , \tag{4}$$

where ω_d is the D-state probability in the deuteron, to obtain $\Delta q = 0.35 \pm 0.05$ for fit II, and $\Delta q = 0.34 \pm 0.05$ for fit III, again somewhat higher than our previous deuteron analysis $\Delta q = 0.30 \pm 0.06$ [7], but in good agreement with the new proton results. For both targets, using the Q^2-independent fit II or the Q^2-dependent fit III makes little difference at $Q^2 = 3$ (GeV/c)^2, but we find Δq (which should be independent of Q^2) to vary less with Q^2 for fit III than for fit II, especially for the deuteron fits.

In summary, the assumption that g_1 and F_1 have approximately the same Q^2-dependence has been found to be consistent with all available data in the deep inelastic region $Q^2 > 1$ (GeV/c)^2, although significant deviations from this assumption are found at lower Q^2. Global fits to the data with and without a possible Q^2 dependence to g_1/F_1 provide a useful parametrization of available data, and validate previous conclusions that the fundamental Bjorken sum rule is satisfied, and that the net quark helicity content of the nucleon is less than expected in the simple relativistic parton model.

We thank the authors of Refs. [18–21] for valuable discussions and for sending numerical results of their calculations.

References

[1] SLAC E80, M. J. Alguard et al., Phys. Rev. Lett. 37 (1976) 1261; 41 (1978) 70.

[2] SLAC E130, G. Baum et al., Phys. Rev. Lett. 51 (1983) 1135.

[3] EMC, J. Ashman et al., Phys. Lett. B206 (1988) 364; Nucl. Phys. B328 (1989) 1.

[4] SMC, D. Adams et al., Phys. Lett. B329 (1994) 399.

[5] SLAC E143, K. Abe et al., Phys. Rev. Lett. 74 (1995) 346.

[6] SMC, D. Adams et al., Report No. CERN–PPE–95–097 (June 1995).

[7] SLAC E143, K. Abe et al., Phys. Rev. Lett. 75 (1995) 25.

[8] SLAC E142, P. L. Anthony et al., Phys. Rev. Lett. 71 (1993) 959.

[9] J. Ellis and R. Jaffe, Phys. Rev. D 9 (1974) 1444; D 10 (1974) 1669 (E).

[10] J. D. Bjorken, Phys. Rev. 148 (1966) 1467; Phys. Rev. D 1 (1970) 1376.

[11] S. A. Larin and J.A.M. Vermaseren, Phys. Lett. B259 (1991) 345 and references therein.

[12] G. Altarelli and G. Parisi, Nucl. Phys. B126 (1977) 298; V. N. Gribov and L. N. Lipatov, Yad. Fiz. 15 (1972) 781 [Sov. J. Nucl. Phys. 15 (1972) 438].

[13] NMC, P. Amaudruz et al., Phys. Lett. B295 (1992) 159.

[14] L. W. Whitlow et al., Phys. Lett. B250 (1990) 193.

[15] S. J. Brodsky, M. Burkardt, and I. Schmidt, Nucl. Phys. B441 (1995) 197.

[16] G. Altarelli, P. Nason, and G. Ridolfi, Phys. Lett. B320 (1994) 152.

[17] E. B. Zijlstra and W. L. van Neerven, Nucl. Phys. B417 (1994) 61; R. Mertig and W. L. van Neervan, Univ. Leiden INLO–PUB–6/95 and NIKHEF–H/95–031 (1995).

[18] T. Gehrmann and W. J. Stirling, Z. Phys. C65 (1995) 461.

[19] B. Ehrnsperger and A. Schäfer, Report No. UFTP/370/1994 (1994).

[20] R. D. Ball, S. Forte, and G. Ridolfi, Nucl. Phys. B444 (1995) 287; and CERN–TH/95–266 (1955).

[21] M. Glück, E. Reya, M. Stratmann, and W. Vogelsang, Reports No. DO–TH–95/13 and RAL–TR–95–042 (August 1995).

[22] I. I. Balitsky, V. M. Braun and A. V. Kolesnichenko, Phys. Lett. B242 (1990) 245; B318 (1993) 648 (E); X. Ji and P. Unrau, Phys. Lett. B333 (1994), 228; E. Stein, P. Cornicki, L. Mankiewicz, A. Schafer, Phys. Lett. B353 (1995) 107.

[23] S. Wandzura and F. Wilczek, Phys. Lett. B72 (1977)195.

[24] SLAC E143, K. Abe et al., Report No. SLAC–PUB–95–6982 (1995), submitted to Phys. Rev. Lett.

[25] T. V. Kuchto and N. M. Shumeiko, Nucl. Phys. B219 (1983) 412; I. V. Akusevich and N. M. Shumeiko, J. Phys. G 20 (1994) 513; Y. S. Tsai, Report No. SLAC–PUB–848 (1971); Y. S. Tsai, Rev. Mod. Phys. 46 (1974) 815.

[26] Particle Data Group, L. Montanet et al., Phys. Rev. D 50 (1994) 1173.

[27] F. E. Close and R. G. Roberts, Phys. Lett. B316 (1993) 165.

[28] S. A. Larin, Phys. Lett. B334 (1994) 192.

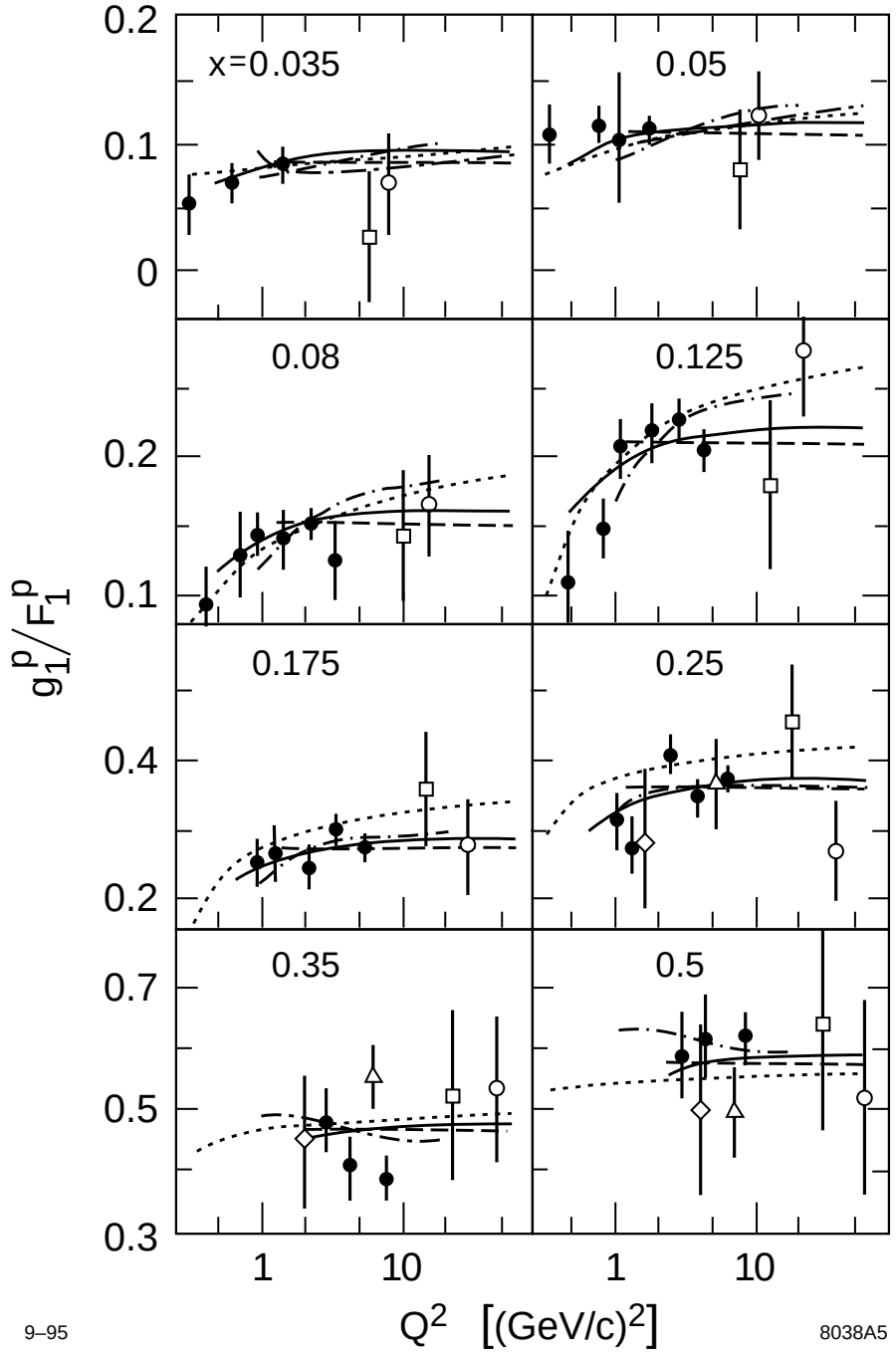

Figure 1. Ratios g_1^p/F_1^p extracted from experiments assuming the g_2^{WW} model for g_2. The errors are statistical only. Data are from this experiment (solid circles), SLAC E80 [1] (diamonds), SLAC E130 [2] (triangles), EMC [3] and SMC [4] (open circles). The dashed and solid curves correspond to global fits II (g_1^p/F_1^p Q^2-independent) and III (g_1^p/F_1^p Q^2-dependent) in Table I, respectively. Representative NLO pQCD fits from Refs. [20] [21] are shown as the dot-dashed and dotted curves, respectively.

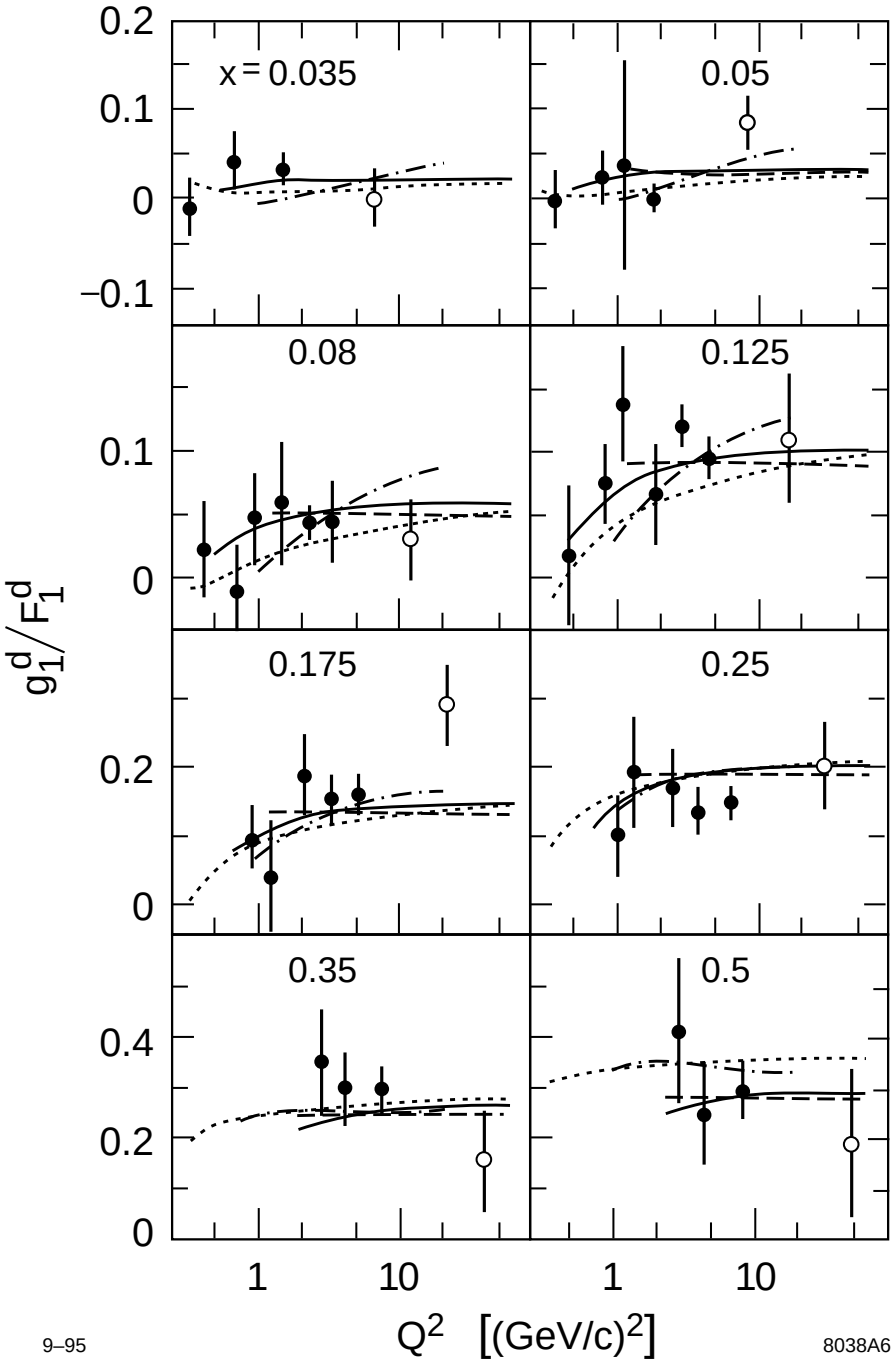

Figure 2. Ratios g_1^d/F_1^d from this experiment (solid circles) and SMC [6] (open circles). The curves are as in Fig. 1.

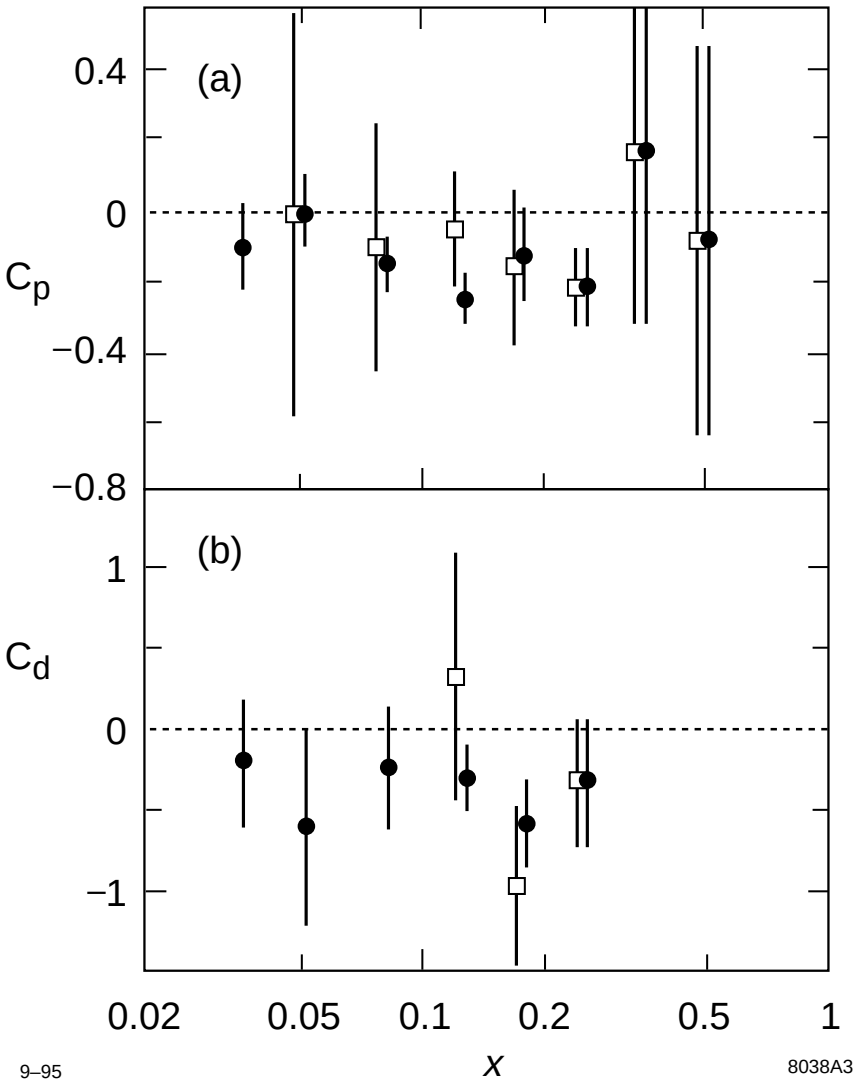

Figure 3. Coefficients C for fits to g_1/F_1 at fixed x of the form $a(1+C/Q^2)$ for (a) proton and (b) deuteron. Solid circles are fits to all data [$Q^2 > 0.3$ (GeV/c)^2], and open squares are fits only to data with $Q^2 > 1$ (GeV/c)^2.

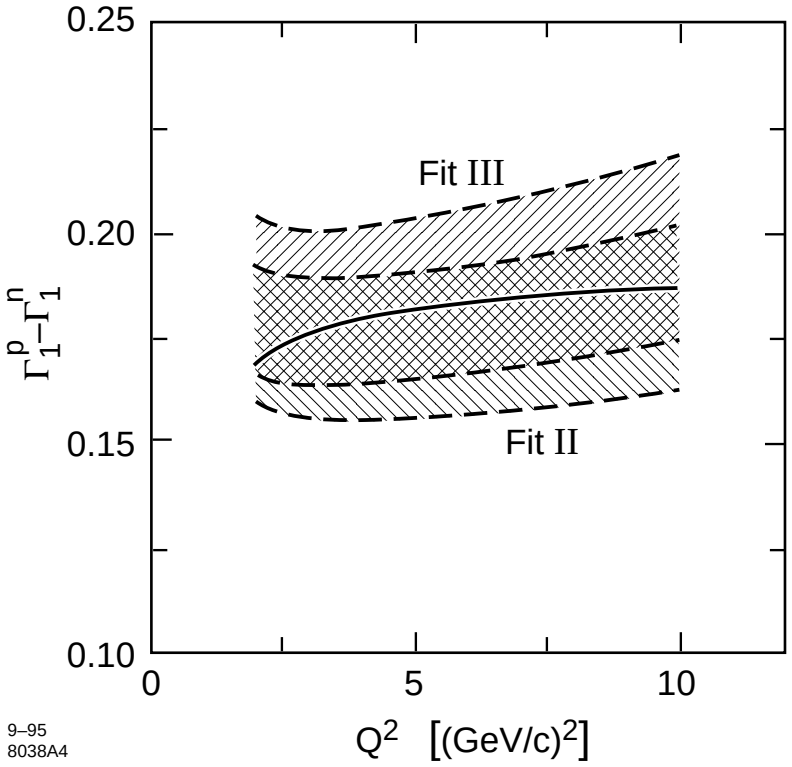

Figure 4. Evaluations of $\Gamma_1^p - \Gamma_1^n$ from the Q^2-independent fits II (lower band) and Q^2-dependent fits III (upper band) listed in Table I. The errors include both statistical and systematic contributions and are indicated by the widths of the bands. The solid curve is the prediction of the Bjorken sum rule with third-order QCD corrections.

TABLE I. Coefficients for fits to all available data with $Q^2 > Q^2_{\rm min}$ of the form $ax^\alpha(1+bx+cx^2)[1+Cf(Q^2)]$, along with the χ^2 for the indicated number of degrees of freedom, calculated with statistical errors only. Fits to IV are to g_1/F_1, while fit V is to A_1.

fit to	$Q^2_{\rm min}$	$f(Q^2)$	α	a	b	c	C	χ^2	d.f.
I. g_1^p/F_1^p	0.3	none	0.50	0.380	4.767	-4.812	0	64	59
II. g_1^p/F_1^p	1.0	none	0.56	0.513	2.948	-3.242	0	40	48
III. g_1^p/F_1^p	0.3	$1/Q^2$	0.50	0.455	3.533	-3.677	-0.140	48	58
IV. g_1^p/F_1^p	0.3	$\ln(1/Q^2)$	0.56	0.487	2.422	-2.717	-0.080	55	58
V. A_1^p	0.3	$1/Q^2$	0.56	0.590	1.871	-1.028	-0.160	51	58
I. g_1^d/F_1^d	0.3	none	1.54	2.760	-1.941	1.072	0	61	45
II. g_1^d/F_1^d	1.0	none	1.48	2.532	-1.908	1.051	0	54	34
III. g_1^d/F_1^d	0.3	$1/Q^2$	1.44	2.612	-1.946	1.109	-0.300	56	44
IV. g_1^d/F_1^d	0.3	$\ln(1/Q^2)$	1.46	2.063	-2.015	1.175	-0.140	58	44
V. A_1^d	0.3	$1/Q^2$	1.46	2.802	-2.125	1.549	-0.320	56	44

TABLE II. Results for g_1^p/F_1^p and g_1^d/F_1^d from this experiment, extracted assuming the g_2^{WW} model for g_2. Both statistical and total systematic errors are listed. The boundaries between the x bins are at 0.03, 0.04, 0.06, 0.1, 0.15, 0.2, 0.3, 0.4, and 0.6.

x	$\langle Q^2 \rangle$ (GeV/c)^2	E (GeV)	$(g_1^p/F_1^p) \pm \text{stat} \pm \text{syst}$	$(g_1^d/F_1^d) \pm \text{stat} \pm \text{syst}$
0.035	0.32	9.7	$0.053 \pm 0.022 \pm 0.021$	$-0.020 \pm 0.031 \pm 0.009$
0.035	0.65	16.2	$0.069 \pm 0.014 \pm 0.011$	$0.039 \pm 0.035 \pm 0.030$
0.035	1.45	29.1	$0.082 \pm 0.014 \pm 0.008$	$0.033 \pm 0.015 \pm 0.011$
0.050	0.37	9.7	$0.110 \pm 0.023 \pm 0.024$	$0.004 \pm 0.033 \pm 0.010$
0.050	0.79	16.2	$0.117 \pm 0.014 \pm 0.013$	$0.023 \pm 0.030 \pm 0.017$
0.050	1.14	16.2	$0.107 \pm 0.051 \pm 0.013$	$0.038 \pm 0.116 \pm 0.014$
0.050	1.82	29.1	$0.113 \pm 0.011 \pm 0.008$	$-0.001 \pm 0.012 \pm 0.008$
0.080	0.42	9.7	$0.095 \pm 0.026 \pm 0.027$	$0.031 \pm 0.038 \pm 0.012$
0.080	0.71	9.7	$0.129 \pm 0.029 \pm 0.024$	$-0.010 \pm 0.042 \pm 0.010$
0.080	0.95	16.2	$0.144 \pm 0.015 \pm 0.016$	$0.048 \pm 0.034 \pm 0.012$
0.080	1.48	16.2	$0.140 \pm 0.020 \pm 0.014$	$0.059 \pm 0.047 \pm 0.011$
0.080	2.33	29.1	$0.150 \pm 0.010 \pm 0.011$	$0.044 \pm 0.012 \pm 0.006$
0.080	3.38	29.1	$0.131 \pm 0.028 \pm 0.011$	$0.039 \pm 0.031 \pm 0.007$
0.125	0.47	9.7	$0.110 \pm 0.037 \pm 0.031$	$0.022 \pm 0.055 \pm 0.016$
0.125	0.85	9.7	$0.150 \pm 0.020 \pm 0.025$	$0.073 \pm 0.030 \pm 0.012$
0.125	1.13	16.2	$0.209 \pm 0.022 \pm 0.019$	$0.138 \pm 0.044 \pm 0.013$
0.125	1.90	16.2	$0.221 \pm 0.019 \pm 0.015$	$0.066 \pm 0.039 \pm 0.009$
0.125	2.94	29.1	$0.227 \pm 0.014 \pm 0.015$	$0.121 \pm 0.017 \pm 0.007$
0.125	4.42	29.1	$0.203 \pm 0.014 \pm 0.013$	$0.095 \pm 0.017 \pm 0.007$
0.175	0.95	9.7	$0.254 \pm 0.032 \pm 0.026$	$0.107 \pm 0.047 \pm 0.014$
0.175	1.24	16.2	$0.265 \pm 0.040 \pm 0.024$	$0.040 \pm 0.081 \pm 0.017$
0.175	2.20	16.2	$0.244 \pm 0.029 \pm 0.019$	$0.189 \pm 0.059 \pm 0.012$
0.175	3.37	29.1	$0.297 \pm 0.025 \pm 0.018$	$0.155 \pm 0.031 \pm 0.011$
0.175	5.33	29.1	$0.270 \pm 0.019 \pm 0.016$	$0.165 \pm 0.023 \pm 0.009$
0.250	1.02	9.7	$0.315 \pm 0.038 \pm 0.027$	$0.105 \pm 0.058 \pm 0.015$
0.250	1.33	16.2	$0.281 \pm 0.039 \pm 0.031$	$0.196 \pm 0.080 \pm 0.025$
0.250	2.52	16.2	$0.411 \pm 0.026 \pm 0.024$	$0.173 \pm 0.054 \pm 0.017$
0.250	3.77	29.1	$0.348 \pm 0.025 \pm 0.022$	$0.138 \pm 0.032 \pm 0.015$
0.250	6.42	29.1	$0.373 \pm 0.017 \pm 0.021$	$0.151 \pm 0.021 \pm 0.013$
0.350	2.80	16.2	$0.480 \pm 0.050 \pm 0.029$	$0.350 \pm 0.104 \pm 0.023$
0.350	4.14	29.1	$0.405 \pm 0.054 \pm 0.027$	$0.300 \pm 0.072 \pm 0.020$
0.350	7.50	29.1	$0.391 \pm 0.033 \pm 0.027$	$0.298 \pm 0.042 \pm 0.018$
0.500	2.97	16.2	$0.590 \pm 0.070 \pm 0.033$	$0.411 \pm 0.141 \pm 0.028$
0.500	4.38	29.1	$0.617 \pm 0.069 \pm 0.034$	$0.246 \pm 0.094 \pm 0.025$
0.500	8.36	29.1	$0.629 \pm 0.038 \pm 0.034$	$0.293 \pm 0.051 \pm 0.022$